Available online at www.sciencedirect.com
SCIENCE DIRECT
Computers and Structures 84 (2006) 978–990
Computers & Structures
www.elsevier.com/locate/compstruc

Stability of composite thin-walled beams with shear deformability

Víctor H. Cortínez *, Marcelo T. Piovan

Grupo de Análisis de Sistemas Mecánicos, Universidad Tecnológica Nacional (FRBB) 11 de Abril 461, 8000, Bahía Blanca, Argentina

Received 14 January 2005; accepted 9 February 2006

Abstract

In this paper, a theoretical model is developed for the stability analysis of composite thin-walled beams with open or closed cross-sections. The present model incorporates, in a full form, the shear flexibility (bending and non-uniform warping), featured in a consistent way by means of a linearized formulation based on the Reissner's Variational Principle. The model is developed using a non-linear displacement field, whose rotations are based on the rule of semi-tangential transformation. This model allows to study the buckling and lateral stability of composite thin-walled beam with general cross-section. A finite element with two-nodes and fourteen-degrees-of-freedom is developed to solve the governing equations. Numerical examples are given to show the importance of the shear flexibility on the stability behavior of this type of structures.

Keywords: Thin-walled; Composite-beam; Buckling; Shear flexibility; Reissner's Principle

1. Introduction

Slender composite structures are increasingly used in many applications of aeronautical, mechanical, naval and even civil engineering industries. The composite materials have many advantages that motivate their use in structural applications. The most well-known features of composite materials are their high strength and stiffness to weight ratio, good corrosion resistance, enhanced fatigue life and low thermal expansion among others [1]. Many structural members are constructed in the form of thin-walled beams. Accordingly, many research activities have been conducted toward the development of theoretical and computational methods for the analysis of the aforementioned structural members.

The structural analysis of isotropic thin-walled open beams is appropriately performed by means of the Vlasov's theory. This theory incorporates the warping deformation, which is a very important effect in these types of beams [2]. In the middle 80s, Bauld and Tzeng [3] introduced an extension of the Vlasov's theory for composite materials. Recently, Ghorbanpoor and Omidvar [4] introduced new equivalent moduli of elasticity and rigidity to allow decoupling (in an approximate form) of Bauld and Tzeng equations. This simplified approach yields nearly the same numerical values obtained with the theory of Bauld and Tzeng. Massa and Barbero [5] proposed a strength-of-materials formulation for static analysis of composite thin-walled beams. A study on the location of shear center was performed by Pollock et al. [6].

Since the middle nineties many authors have focused their research efforts in proposing mathematical models to study the instability behavior of composite thin-walled beams. Shearbourne and Kabir [7] analyzed the shear effect in connection with the lateral stability of composite I-section beams. Godoy et al. [8] developed a mathematical model for I-section composite beams considering shear effects and cross-sectional distortion for interactive buckling analysis. Omidvar [9] analyzed shear flexibility associated to bending and introduced new formulae for shear coefficients. On the basis of earlier works of Librescu and Song [10], Bhaskar and Librescu [11] introduced a model

* Corresponding author. Tel.: +54 291 4555220; fax: +54 291 4555311.
E-mail address: vcortine@frbb.utn.edu.ar (V.H. Cortínez).

0045-7949/$ - see front matter © 2006 Elsevier Ltd. All rights reserved.
doi:10.1016/j.compstruc.2006.02.017

for the buckling analysis under axial compression of composite box-beam with extension-twisting coupling. In the last three references, it may be seen an interesting analysis about the influence of secondary warping on the mechanics of composite thin-walled beams. Recently, Lee et al. [12–14] developed extended models of the Bauld and Tzeng's theory, in order to perform lateral buckling analysis of composite laminated I-section and channel-section beams.

The above-mentioned papers neglect the shear flexibility or at least do not consider the shear flexibility in a full form, i.e. shear flexibility due to bending and shear flexibility due to non-uniform warping. It has to be noted that the aforementioned works of Massa and Barbero [5], Pollock et al. [6], Librescu and Song [10], Bhaskar and Librescu [11] and Omidvar [9] consider the shear flexibility due to bending, however none of them take into account the shear flexibility due to non-uniform warping. These two effects may play an important role in the prediction of natural frequencies and buckling loads of thin-walled beams (for both isotropic and composite materials as shown by Cortínez et al. [15,16]).

According to authors' knowledge there are a few papers that take into account the shear flexibility effect in a full form on the mechanics of composite materials. The first one is that of Wu and Sun [17], however in their paper these authors obtained only natural frequencies and emphasis was given in showing the effectiveness of the developed finite element. Recently, Kollár [18] and Sapkás and Kollár [19] explored the buckling behavior of composite columns by means of an analytical study including full-shear flexibility. However, in these last works, no general loading conditions were involved and the governing equations were obtained by means of classical (equilibrium) approaches [20,21].

Recently, the authors have developed a new model of composite thin-walled beams, based on the use of the Hellinger–Reissner principle, that considers shear flexibility in a full form, general cross-section shapes and symmetric balanced or especially orthotropic laminates. On the other hand, it was formulated taking into account the existence of a uniform distribution of initial axial force and bending moments.

The model was applied for analyzing vibration and buckling problems.

This paper introduces a generalization of the aforementioned model in order to consider the existence of an arbitrary state of initial stresses, including general off-axis loadings.

To do this, a generalized displacement field is employed which includes non-linear terms based on the rule of semi-tangential rotations introduced by Argyris et al. [22,23].

This displacement field enhances the one employed by the authors in a previous work [16]. In these circumstances the functional is extended to account for the new displacement terms as well as generalized initial volume forces and initial off-axis forces that were not considered in the previous work.

The aforementioned non-linear terms play an important role in general buckling problems. In fact, in the context of isotropic thin-walled beams, Kim et al. [24,25] demonstrated that the omission of these terms may lead to inaccurate results of buckling loads for some cases, especially when an off-axis loading is considered.

A non-locking finite element with fourteen degrees of freedom is developed for analyzing stability under both axial and lateral loads. Parametric studies with different cross-sections and laminate stacking sequences are carried out.

2. Theory

2.1. Assumptions

A composite thin-walled beam with an arbitrary cross-section is considered (Fig. 1a and b). The points of the structural member are referred to the Cartesian co-ordinate system $\{x, y, z\}$ located at the geometric center, where the x-axis is parallel to the longitudinal axis of the beam, while

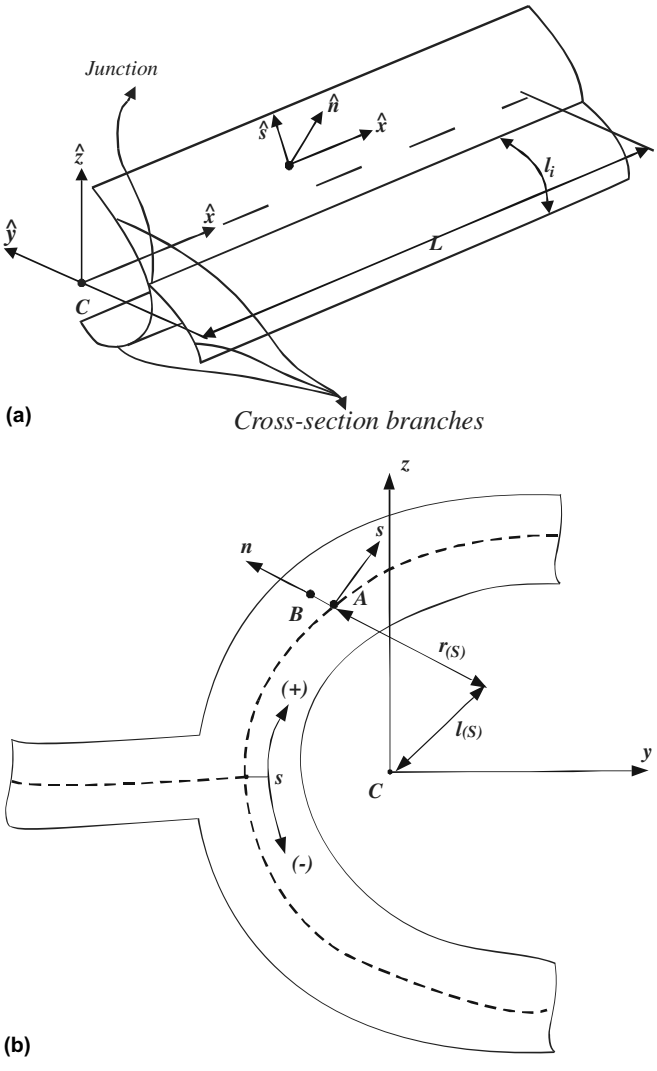

Fig. 1. Geometry of the beam.

y and z are the axes of the cross-section, but not necessarily the principal ones. The co-ordinates corresponding to points lying on the middle line are denoted with Y and Z. In addition, a circumferential co-ordinate s and a normal co-ordinate n are introduced on the middle contour of the cross-section.

The present structural model is based on the following assumptions: (1) the cross-section contour is rigid in its own plane; (2) the warping distribution is assumed to be given by the Saint-Venant function for isotropic beams; (3) shell force (N_{ss}) and moment (M_{ss}) resultants corresponding to the circumferential stress σ_{ss} and the inter-laminar force resultant (N_{sn}) corresponding to inter-laminar strain γ_{ns} are neglected; (4) the curvature at any point of the shell is neglected; (5) twisting curvature of the shell is expressed according to the classical plate theory, but bending curvature is expressed according to the first-order shear deformation theory; in fact, bending shear strain of the wall is incorporated; (6) the laminate stacking sequence is assumed to be symmetric and balanced, or specially orthotropic [1] (the corresponding constitutive equations for the shell stress resultants are given in Appendix I); (7) the displacement field is considered to be represented by a linear component and a second-order component based on the semi-tangential rotations introduced by Argyris [22,23]; (8) higher-order strain components due to second-order displacements are neglected in the Green–Lagrange strain tensor; (9) higher-order shell stress resultants (i.e. depending on n^k, where $k > 1$) are neglected.

2.2. Variational formulation

Taking into account the adopted assumptions, the Hellinger–Reissner principle for a composite shell may be presented in the following form: [26]:

$$\begin{aligned}
&\int\int \left[N_{xx}\delta\varepsilon^{\mathrm{L}}_{xx} + M_{xx}\delta\kappa^{\mathrm{L}}_{xx} + N_{xs}\delta\gamma^{\mathrm{L}}_{xs} + M_{xs}\delta\kappa^{\mathrm{L}}_{xs} + N_{xn}\delta\gamma^{\mathrm{L}}_{xn}\right]\mathrm{d}s\,\mathrm{d}x \\
&+\int\int \left[N^0_{xx}\delta\varepsilon^{\mathrm{NL}}_{xx} + M^0_{xx}\delta\kappa^{\mathrm{NL}}_{xx} + N^0_{xs}\delta\gamma^{\mathrm{NL}}_{xs} + M^0_{xs}\delta\kappa^{\mathrm{NL}}_{xs} + N^0_{xn}\delta\gamma^{\mathrm{NL}}_{xn}\right]\mathrm{d}s\,\mathrm{d}x \\
&-\int\int \left[\overline{T}_x\delta u^{\mathrm{L}}_x + \overline{T}_s\delta u^{\mathrm{L}}_s + \overline{T}_n\delta u^{\mathrm{L}}_n\right]\mathrm{d}s\,\mathrm{d}x \\
&-\int\int\int \left[\overline{X}_x\delta u^{\mathrm{L}}_x + \overline{X}_s\delta u^{\mathrm{L}}_s + \overline{X}_n\delta u^{\mathrm{L}}_n\right]\mathrm{d}s\,\mathrm{d}n\,\mathrm{d}x \\
&-\int\int \left[\overline{T}^0_x\delta u^{\mathrm{NL}}_x + \overline{T}^0_s\delta u^{\mathrm{NL}}_s + \overline{T}^0_n\delta u^{\mathrm{NL}}_n\right]\mathrm{d}s\,\mathrm{d}x \\
&-\int\int\int \left[\overline{X}^0_x\delta u^{\mathrm{NL}}_x + \overline{X}^0_s\delta u^{\mathrm{NL}}_s + \overline{X}^0_n\delta u^{\mathrm{NL}}_n\right]\mathrm{d}s\,\mathrm{d}n\,\mathrm{d}x \\
&-\left[\int \left(\overline{N}_{xx}\delta\overline{U}^{\mathrm{L}}_x + \overline{M}_{xx}\delta\overline{\phi}_{xx} + \overline{N}_{xs}\delta\overline{U}^{\mathrm{L}}_s\right.\right. \\
&\left.\left. + \overline{M}_{xs}\delta\overline{\phi}_{ss} + \overline{N}_{xn}\delta\overline{U}^{\mathrm{L}}_n\right)\mathrm{d}s\right]^{x=L}_{x=0} = 0
\end{aligned} \tag{1a}$$

$$\begin{aligned}
&\int\int \left[\left(\varepsilon^{\mathrm{L}}_{xx} - \frac{N_{xx}}{A_{11}}\right)\delta N_{xx} + \left(\gamma^{\mathrm{L}}_{xs} - \frac{N_{xs}}{A_{66}}\right)\delta N_{xs} + \left(k^{\mathrm{L}}_{xs} - \frac{M_{xs}}{D_{66}}\right)\delta M_{xs}\right]\mathrm{d}s\,\mathrm{d}x \\
&+\int\int \left[\left(k^{\mathrm{L}}_{xx} - \frac{M_{xx}}{D_{11}}\right)\delta M_{xx} + \left(\gamma^{\mathrm{L}}_{xn} - \frac{N_{xn}}{A^{(H)}_{55}}\right)\delta N_{xn}\right]\mathrm{d}s\,\mathrm{d}x = 0
\end{aligned} \tag{1b}$$

where N_{xx}, N_{xs}, M_{xx}, M_{xs} and N_{xn} are shell stress resultants defined according to the following expressions:

$$N_{xx} = \int_{-e/2}^{e/2}\sigma_{xx}\,\mathrm{d}n, \quad M_{xx} = \int_{-e/2}^{e/2}(\sigma_{xx}n)\,\mathrm{d}n,$$

$$M_{xs} = \int_{-e/2}^{e/2}(\sigma_{xs}n)\,\mathrm{d}n \tag{2a, b, c}$$

$$N_{xs} = \int_{-e/2}^{e/2}\sigma_{xs}\,\mathrm{d}n, \quad N_{xn}\int_{-e/2}^{e/2}\sigma_{xn}\,\mathrm{d}n \tag{2d, e}$$

Initial shell stress resultants are denoted with the superscript '$\bullet^0$' and the applied shell stress resultants on the boundaries are denoted as '$\overline{\bullet}$'. $\overline{T}_x$, $\overline{T}_s$ and $\overline{T}_n$ are applied forces per unit area in x, s and n directions, respectively, while $\overline{X}_x$, $\overline{X}_s$ and $\overline{X}_n$ are forces per unit volume in x, s and n directions, respectively. The strain components $\varepsilon^{\mathrm{L}}_{xx}, \gamma^{\mathrm{L}}_{xs}, \gamma^{\mathrm{L}}_{xn}, \kappa^{\mathrm{L}}_{xx}, \kappa^{\mathrm{L}}_{xs}$ and $\varepsilon^{\mathrm{NL}}_{xx}, \gamma^{\mathrm{NL}}_{xs}, \gamma^{\mathrm{NL}}_{xn}, \kappa^{\mathrm{NL}}_{xx}, \kappa^{\mathrm{NL}}_{xs}$ are the first- and second-order shell strains which are defined later in terms of the shell displacements $\overline{U}^{\mathrm{L}}_x, \overline{U}^{\mathrm{L}}_s, \overline{U}^{\mathrm{L}}_n$ and shell rotations $\overline{\phi}_{xx}, \overline{\phi}_{ss}$, see Fig. 2. Finally, $u^{\mathrm{L}}_x, u^{\mathrm{L}}_s, u^{\mathrm{L}}_n$ and $u^{\mathrm{NL}}_x, u^{\mathrm{NL}}_s, u^{\mathrm{NL}}_n$ are linear and non-linear components of the displacement field with respect to the contour co-ordinate system. In the following pages, superscripts "L" and "NL" identifies the linear and second-order components of the displacement field and shell strains, respectively.

It should be noted that, in Eqs. (1), the stress resultants and the displacements are variationally independent quantities. Expressions (1a) and (1b) represent the variational forms of the equilibrium and compatibility equations, respectively.

2.3. Kinematic expressions

The displacement field, compatible with assumptions (1), (2) and (7), is adopted in the form [27]:

$$u^{\mathrm{L}}_x(x,t) = u_{xc}(x,t) - y\theta_z(x,t) - z\theta_y(x,t) - \omega\theta_x(x,t) \tag{3a}$$

$$u^{\mathrm{L}}_y(x,t) = u_{yc}(x,t) - z\phi_x(x,t) \tag{3b}$$

$$u^{\mathrm{L}}_z(x,t) = u_{zc}(x,t) + y\phi_x(x,t) \tag{3c}$$

$$u^{\mathrm{NL}}_x(x,t) = \frac{1}{2}\left[z\phi_x(x,t)\theta_z(x,t) - y\phi_x(x,t)\theta_y(x,t)\right] \tag{3d}$$

$$u^{\mathrm{NL}}_y(x,t) = -\frac{y}{2}\left[(\phi_x(x,t))^2 + \theta_z(x,t)^2\right] - \frac{z}{2}\theta_z(x,t)\theta_y(x,t) \tag{3e}$$

$$u^{\mathrm{NL}}_z(x,t) = -\frac{z}{2}\left[(\phi_x(x,t))^2 + \left(\theta_y(x,t)\right)^2\right] - \frac{y}{2}\theta_z(x,t)\theta_y(x,t) \tag{3f}$$

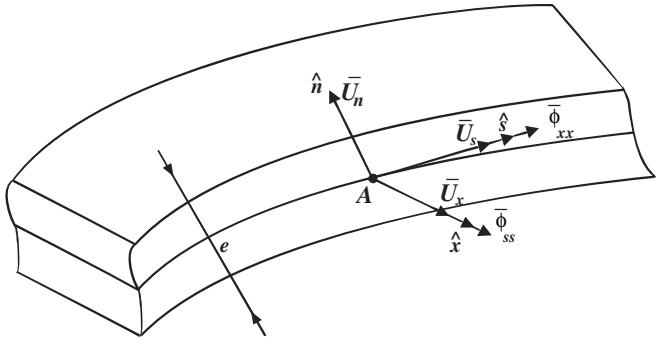

Fig. 2. Displacements defined with respect to the wall co-ordinate system.

where

$$y(s,n) = Y(s) - n\frac{dZ}{ds}, \quad z(s,n) = Z(s) + n\frac{dY}{ds} \tag{4}$$

In expressions (3), u_{xc}, u_{yc}, u_{zc} are the displacements of the centroid, ϕ_x is the torsional rotation, θ_y and θ_z are the bending rotations. The variable θ_x measures the warping intensity. When the non-linear components (3d)–(3f) are neglected, the displacement field is equivalent to that proposed in reference [16].

The warping function can be written in the following form:

$$\omega(s,n) = \omega_p(s) + \omega_s(s,n) \tag{5}$$

where ω_p and ω_s are the contour warping function and the thickness warping function, respectively. They are defined in the form [27]:

$$\omega_p(s) = \frac{1}{S}\left[\int_0^S \left(\int_{s_0}^s [r(s)+\psi(s)]ds\right)ds\right] - \int_{s_0}^s [r(s)+\psi(s)]ds$$
$$\omega_s(s,n) = nl(s) \tag{6a,b}$$

with

$$r(s) = Z(s)\frac{dY}{ds} - Y(s)\frac{dZ}{ds},$$
$$l(s) = Y(s)\frac{dY}{ds} + Z(s)\frac{dZ}{ds} \tag{7a,b}$$

In expression (6a), ψ is the shear strain in the middle line, obtained by means of the Saint-Venant theory of pure torsion, and normalized with respect to $d\phi_x/dx$, as can be seen in reference [27] for composite beams or in Krenk and Gunneskov [28] for isotropic beams. For the case of open sections, it can be proved that $\psi = 0$.

The displacements with respect to the curvilinear system are obtained by means of the following geometric transformation:

$$\overline{U}_x^{\mathrm{L}} = u_x^{\mathrm{L}}(x,s,0),$$
$$\overline{U}_x^{\mathrm{NL}} = u_x^{\mathrm{NL}}(x,s,0) \tag{8a,b}$$

$$\overline{U}_s^{\mathrm{L}} = u_y^{\mathrm{L}}(x,s,0)\frac{dY}{ds} + u_z^{\mathrm{L}}(x,s,0)\frac{dZ}{ds},$$
$$\overline{U}_s^{\mathrm{NL}} = u_y^{\mathrm{NL}}(x,s,0)\frac{dY}{ds} + u_z^{\mathrm{NL}}(x,s,0)\frac{dZ}{ds} \tag{8c,d}$$

$$\overline{U}_n^{\mathrm{L}} = -u_y^{\mathrm{L}}(x,s,0)\frac{dZ}{ds} + u_z^{\mathrm{L}}(x,s,0)\frac{dY}{ds},$$
$$\overline{U}_n^{\mathrm{NL}} = -u_y^{\mathrm{NL}}(x,s,0)\frac{dZ}{ds} + u_z^{\mathrm{NL}}(x,s,0)\frac{dY}{ds} \tag{8e,d}$$

$$\overline{\phi}_{xx} = \frac{\partial u_{xc}}{\partial n}, \quad \overline{\phi}_{ss} = \frac{\partial}{\partial n}\left(u_y^{\mathrm{L}}\frac{dY}{ds} + u_z^{\mathrm{L}}\frac{dZ}{ds}\right) \tag{8f,g}$$

By introducing the displacements (8) into the definitions of strain components [16], and taking into account hypotheses (1)–(9), one can obtain the following expressions for the first $(\varepsilon_{xx}, \gamma_{xs}, \gamma_{xn})$ and second $(\eta_{xx}, \eta_{xs}, \eta_{xn})$ order strain components:

$$\varepsilon_{xx} = \varepsilon_{xx}^{\mathrm{L}} + n\kappa_{xx}^{\mathrm{L}}, \quad \gamma_{xs} = \gamma_{xs}^{\mathrm{L}} + n\kappa_{xs}^{\mathrm{L}}, \quad \gamma_{xn} = \gamma_{xn}^{\mathrm{L}} \tag{9a,b,c}$$
$$\eta_{xx} = \varepsilon_{xx}^{\mathrm{NL}} + n\kappa_{xx}^{\mathrm{NL}}, \quad \eta_{xs} = \gamma_{xs}^{\mathrm{NL}} + n\kappa_{xs}^{\mathrm{NL}}, \quad \eta_{xn} = \gamma_{xn}^{\mathrm{NL}} \tag{9d,e,f}$$

where

$$\varepsilon_{xx}^{\mathrm{L}} = u'_{xc} - Y(s)\theta'_z - Z(s)\theta'_y - \omega_P(s)\theta'_x,$$
$$\kappa_{xx}^{\mathrm{L}} = \theta'_z\frac{dZ}{ds} - \theta'_y\frac{dY}{ds} - \theta'_x l(s) \tag{10a,b}$$

$$\gamma_{xs}^{\mathrm{L}} = (u'_{yc} - \theta_z)\frac{dY}{ds} + (u'_{zc} - \theta_y)\frac{dZ}{ds} - (\phi'_x - \theta_x)(r+\psi) + \phi'_x\psi,$$
$$\kappa_{xs}^{\mathrm{L}} = 2\phi'_z \tag{10c,d}$$

$$\gamma_{xn}^{\mathrm{L}} = -(u'_{yc} - \theta_z)\frac{dZ}{ds} + (u'_{zc} - \theta_y)\frac{dY}{ds} + (\phi'_x - \theta_x)l(s) \tag{10e}$$

$$\varepsilon_{xx}^{\mathrm{NL}} = \frac{1}{2}\left\{u'^2_{yc} + u'^2_{yc} + \phi'^2_{yc}(Y^2+Z^2) + Z[-2\phi'_x u'_{yc} + (\phi_x\theta_z)'] + Y\left[2\phi'_x u'_{zc} - (\phi_x\theta_y)'\right]\right\} \tag{10f}$$

$$\kappa_{xx}^{\mathrm{NL}} = \frac{1}{2}\left\{(\phi_x\theta_y)'\frac{dZ}{ds} + (\phi_x\theta_z)'\frac{dY}{ds} - 2\phi'_x\left[u'_{yc}\frac{dY}{ds} + u'_{zc}\frac{dZ}{ds} - \phi'_x r(s)\right]\right\} \tag{10g}$$

$$\gamma_{xs}^{\mathrm{NL}} = \frac{1}{2}\left\{\phi_x\left(\theta_z\frac{dZ}{ds} - \theta_y\frac{dY}{ds}\right) + r(s)\left(\theta'_y\theta_z - \theta'_z\theta_y\right) - 2(r+\psi)\theta_x\left(\theta'_z Y + \theta'_y Z\right)\right\} + \left\{\phi_x\left(u'_{zc}\frac{dY}{ds} - u'_{yc}\frac{dZ}{ds}\right) - \left(u'_{xc} - \omega_p\theta'_x\right)\left(\theta_y\frac{dZ}{ds} + \theta_z\frac{dY}{ds} - \theta_x(r+\psi)\right)\right\} \tag{10h}$$

$$\gamma_{xn}^{\mathrm{NL}} = \frac{1}{2}\left\{\phi_x\left(\theta_y\frac{dZ}{ds} + \theta_z\frac{dY}{ds}\right) - l(s)\left(\theta'_y\theta_z - \theta'_z\theta_y\right) + 2l(s)\theta_x\left(\theta'_z Y + \theta'_y Z\right)\right\} + \left\{-\phi_x\left(u'_{zc}\frac{dZ}{ds} + u'_{yc}\frac{dY}{ds}\right) + \left(u'_{xc} - \omega_p\theta'_x\right)\left(\theta_z\frac{dZ}{ds} - \theta_y\frac{dY}{ds} - \theta_x l(s)\right)\right\} \tag{10i}$$

$$\kappa_{xs}^{\mathrm{NL}} = \left(\theta'_y\theta_z - \theta'_z\theta_y\right) - (r+\psi)\theta_x\left(\theta'_y\frac{dY}{ds} - \theta'_z\frac{dZ}{ds} + \theta'_x l(s)\right) + l(s)\theta'_x\left(\theta_y\frac{dZ}{ds} + \theta_z\frac{dY}{ds}\right) \tag{10j}$$

In the above expressions $(\bullet)'$ denotes derivation with respect to the x variable.

The first and second terms in expressions (10c) and (10e) may be regarded as the shear strains associated to bending, the third terms correspond to the shear strain due to non-uniform warping and the last term in expression (10c) is the Saint-Venant (or pure torsion) shear strain.

2.4. Equations of motion

Substituting expressions (9) and (10) into Eq. (1a) and integrating with respect to variable s, one can obtain the expression for the virtual work equation given by

$$L_K + L_{KG1} + L_{KG2} + L_P = 0 \tag{11}$$

where

$$L_K = \int_L \left[Q_X \delta u'_{xc} - M_Y \delta\theta'_y - M_Z \delta\theta'_z - B\delta\theta'_x + T_{SV}\delta\phi'_x\right]\mathrm{d}x + \int_L \left[Q_Y \delta\left(u'_{yc} - \theta_z\right) + Q_Z \delta\left(u'_{zc} - \theta_y\right) + T_W \delta\left(\phi'_x - \theta_x\right)\right]\mathrm{d}x \tag{12a}$$

$$\begin{aligned} L_{KG1} = {} & \int_L \left\{\frac{Q_X^{(0)}}{2}\delta\left(u'^2_{zc} + u'^2_{yc}\right) + \frac{P_W^{(0)}}{2}\delta\left(\phi'^2_x\right) + \frac{M_Z^{(0)}}{2}\delta\left[2u'_{zc}\phi'_x - \left(\phi_x\theta_y\right)'\right]\right\}\mathrm{d}x \\ & + \int_L \left\{\frac{M_Y^{(0)}}{2}\delta\left[-2u'_{yc}\phi'_x + \left(\phi_x\theta_z\right)'\right]\right. \\ & \left. + \frac{M_X^{(0)}}{2}\delta\left(\theta'_z\theta_y - \theta'_y\theta_z\right) - T_W^{(0)}\delta\left(u'_{xc}\theta_x\right)\right\}\mathrm{d}x \\ & + \int_L \left\{Q_Y^{(0)}\delta\left(u'_{zc}\phi_x - u'_{xc}\theta_z - \frac{\phi_x\theta_y}{2}\right)\right. \\ & \left. + Q_Z^{(0)}\delta\left(\frac{\phi_x\theta_z}{2} - u'_{xc}\theta_y - \phi_x u'_{yc}\right)\right\}\mathrm{d}x \\ & + \int_L \left\{Q_{YW}^{(0)}\delta\left(\theta'_x\theta_z\right) + Q_{ZW}^{(0)}\delta\left(\theta'_x\theta_y\right) + T_{WW}^{(0)}\delta\left(\theta'_x\theta_x\right)\right. \\ & \left. + T_{WZ}^{(0)}\delta\left(\theta'_y\theta_x\right) + T_{WY}^{(0)}\delta\left(\theta'_z\theta_x\right)\right\}\mathrm{d}x \end{aligned} \tag{12b}$$

$$L_{KG2} = -\int_L \left[\overline{X}_3^{(0)}\delta\theta_z + \overline{X}_5^{(0)}\delta\theta_y + \overline{X}_6^{(0)}\delta\phi_x\right]\mathrm{d}x - \left[\overline{T}_3^{(0)}\delta\theta_z + \overline{T}_5^{(0)}\delta\theta_y + \overline{T}_6^{(0)}\delta\phi_x\right]_{x=0}^{x=L} \tag{12c}$$

$$\begin{aligned} L_P = {} & -\int_L \left[q_1(x,t)\delta u_{xc} + q_3(x,t)\delta\theta_z + q_5(x,t)\delta\theta_y + q_7(x,t)\delta\theta_x\right]\mathrm{d}x \\ & -\int_L \left[q_2(x,t)\delta u_{yc} + q_4(x,t)\delta u_{zc} + q_6(x,t)\delta\phi_x\right]\mathrm{d}x \\ & -\left[\overline{Q}_X\delta u_{xc} + \overline{Q}_Y\delta u_{yc} - \overline{M}_Z\delta\theta_z - \overline{B}\delta\theta_x\right. \\ & \left. + \overline{Q}_Z\delta u_{zc} - \overline{M}_Y\delta\theta_y + \overline{M}_X\delta\phi_x\right]_{x=0}^{x=L} \end{aligned} \tag{12d}$$

In the previous equations the following definitions, for the beam forces have been made:

$$Q_X = \int_S N_{xx}\,\mathrm{d}s, \quad B = \int_S \left[N_{xx}\omega_p(s) + M_{xx}l(s)\right]\mathrm{d}s \tag{13a, b}$$

$$Q_Y = \int_S \left[N_{xs}\frac{\mathrm{d}Y}{\mathrm{d}s} - N_{xn}\frac{\mathrm{d}Z}{\mathrm{d}s}\right]\mathrm{d}s,$$

$$Q_Z = \int_S \left[N_{xs}\frac{\mathrm{d}Z}{\mathrm{d}s} + N_{xn}\frac{\mathrm{d}Y}{\mathrm{d}s}\right]\mathrm{d}s \tag{13c, d}$$

$$M_Y = \int_S \left[N_{xx}Z(s) + M_{xx}\frac{\mathrm{d}Y}{\mathrm{d}s}\right]\mathrm{d}s,$$

$$M_Z = \int_S \left[N_{xx}Y(s) - M_{xx}\frac{\mathrm{d}Z}{\mathrm{d}s}\right]\mathrm{d}s \tag{13e, f}$$

$$T_W = \int_S \{-N_{xs}[r(s) + \psi(s)] + N_{xn}l(s)\}\mathrm{d}s,$$

$$T_{SV} = \int_S \left[N_{xs}\psi(s) - 2M_{xs}\right]\mathrm{d}s \tag{13g, h}$$

$$M_X = T_{SV} + T_W \tag{13i}$$

In the above expressions the integration is carried out over the middle contour perimeter. Q_X is the axial force, M_Y and M_Z are the bending moments, B is the bimoment, Q_Y and Q_Z are the shear forces, T_W is the flexural torsional moment, T_{SV} is the Saint-Venant torsional moment and M_X is the total torsional moment. $\overline{Q}_X, \overline{Q}_Y, \overline{M}_Z, \overline{B}, \overline{Q}_Z, \overline{M}_Y, \overline{M}_X$ correspond to external generalized forces acting at the ends.

The functions $q_i(x,t)$, $i = 1,\ldots,7$, are the generalized applied forces per unit length. $\overline{X}_3^{(0)}, \overline{X}_5^{(0)}, \overline{X}_6^{(0)}$ and $\overline{T}_3^{(0)}, \overline{T}_5^{(0)}, \overline{T}_6^{(0)}$ are functions which condense the initial volume and surface (at the ends) forces, respectively. $Q_X^{(0)}$, $Q_Y^{(0)}, Q_Z^{(0)}, M_X^{(0)}, M_Y^{(0)}, M_Z^{(0)}, T_W^{(0)}$ and $T_{WW}^{(0)}, T_{WY}^{(0)}, T_{WZ}^{(0)}, Q_{YW}^{(0)}, Q_{ZW}^{(0)}$ are initial beam stress resultants and generalized beam stress resultants, respectively. All these entities are extensively described in Appendix II.

One may notice that L_K, L_{KG1}, L_{KG2} and L_P in Eqs. (12) represent the virtual work contributions due to incremental, initial and external forces respectively. It has to be pointed out that the virtual work due to initial external forces, L_{KG2}, would have no meaning if the displacement field were reduced to the linear form. However, this contribution is fundamental in order to solve stability problems with off-axis loadings or general loadings.

It is important to point out that in Eq. (12b) the term corresponding to the initial torsional moment $M_X^{(0)}$, was obtained naturally without amending the functional expression, as it was performed in other works (for example in reference [29]). This fact is due to the adoption of an enhanced displacement field in connection with a more comprehensive strain field, in order to describe the virtual work contribution of initial stresses and forces (see reference [27] for a detailed discussion of this subject, in the context of composite beams).

2.5. Constitutive equations for the beam stress resultants

The shell stress resultants can be derived with a similar approach to the one employed previously by Cortínez and Piovan [16], where the reference axes were parallel to the principal ones and two-poles where employed. However, with the aim to generalize that conception (remember, in this article the axes are located at the geometric center but not necessarily parallel to the principal ones), it is important to use matrix representation for the strain and stress components, in order to avoid excessive algebraic manipulation. Accordingly, the field of shell stress resultants can be assumed in the following way:

$$N_{xx} = e\boldsymbol{C}_{N1}^{\mathrm{T}}\left(\boldsymbol{J}_N^*\right)^{-1}\boldsymbol{Q}_N, \quad M_{xx} = \frac{e^3}{12}\boldsymbol{C}_{N2}^{\mathrm{T}}\left(\boldsymbol{J}_N^*\right)^{-1}\boldsymbol{Q}_N \tag{14a, b}$$

$$N_{xs} = e\boldsymbol{C}_{N3}^{\mathrm{T}}\left(\boldsymbol{J}_T^*\right)^{-1}\boldsymbol{Q}_T, \quad N_{xn} = \frac{e^3}{12}\boldsymbol{C}_{N2}^{\mathrm{T}}\left(\boldsymbol{J}_T^*\right)^{-1}\boldsymbol{Q}_T,$$

$$M_{xs} = \frac{e^3}{12}\boldsymbol{C}_{N5}^{\mathrm{T}}\left(\boldsymbol{J}_T^*\right)^{-1}\boldsymbol{Q}_T \tag{14c, d, e}$$

In case of using a principal-axes and two-pole reference system, expressions (14) can be reduced to simplified forms (see Appendix III). The shell strains can be expressed in the following form:

$$\varepsilon_{xx}^{\mathrm{L}} = \boldsymbol{C}_{N1}^{\mathrm{T}}\boldsymbol{\varepsilon}_N, \quad \boldsymbol{\kappa}_{xx}^{\mathrm{L}} = \boldsymbol{C}_{N2}^{\mathrm{T}}\boldsymbol{\varepsilon}_N \tag{15a, b}$$

$$\gamma_{xn}^{\mathrm{L}} = \boldsymbol{C}_{N2}^{\mathrm{T}}\boldsymbol{\varepsilon}_T, \quad \gamma_{xs}^{\mathrm{L}} = \boldsymbol{C}_{N4}^{\mathrm{T}}\boldsymbol{\varepsilon}_T, \quad \boldsymbol{\kappa}_{xs}^{\mathrm{L}} = \boldsymbol{C}_{N5}^{\mathrm{T}}\boldsymbol{\varepsilon}_T \tag{15c, d, e}$$

In expressions (14) and (15) the following vectors and matrices are introduced:

$$\boldsymbol{Q}_N = \langle Q_X, M_Y, M_Z, B\rangle^{\mathrm{T}},$$

$$\boldsymbol{Q}_T = \langle T_{SV}, Q_Z, Q_Y, T_W\rangle^{\mathrm{T}} \tag{16a, b}$$

$$\boldsymbol{\varepsilon}_N = \left\langle u'_{xc}, -\theta'_y, -\theta'_z, -\theta'_x \right\rangle^{\mathrm{T}},$$

$$\boldsymbol{\varepsilon}_T = \left\langle \phi'_x, \left(u'_{zc} - \theta_y\right), \left(u'_{yc} - \theta_z\right), \left(\phi'_x - \theta_x\right) \right\rangle^{\mathrm{T}} \tag{16c, d}$$

$$\boldsymbol{C}_{N1} = \langle 1, Z(s), Y(s), \omega_P(s)\rangle^{\mathrm{T}},$$

$$\boldsymbol{C}_{N2} = \left\langle 0, \frac{\mathrm{d}Y}{\mathrm{d}s}, -\frac{\mathrm{d}Z}{\mathrm{d}s}, l(s) \right\rangle^{\mathrm{T}} \tag{16e, f}$$

$$\boldsymbol{C}_{N3} = \left\langle \psi, -\overline{\lambda}_y, -\overline{\lambda}_z, -\overline{\lambda}_\omega \right\rangle^{\mathrm{T}},$$

$$\boldsymbol{C}_{N4} = \left\langle \psi, \frac{\mathrm{d}Z}{\mathrm{d}s}, \frac{\mathrm{d}Y}{\mathrm{d}s}, -(r+\psi) \right\rangle^{\mathrm{T}},$$

$$\boldsymbol{C}_{N5} = \langle -2, 0, 0, 0\rangle^{\mathrm{T}} \tag{16g, h, i}$$

$$\boldsymbol{J}_N^* = \begin{bmatrix} J_{11} & 0 & 0 & 0 \\ 0 & J_{22} & J_{23} & J_{24} \\ 0 & J_{23} & J_{33} & J_{34} \\ 0 & J_{24} & J_{34} & J_{44} \end{bmatrix},$$

$$\boldsymbol{J}_T^* = \begin{bmatrix} J_{55} & 0 & 0 & 0 \\ 0 & J_{22} & J_{23} & J_{24} \\ 0 & J_{23} & J_{33} & J_{34} \\ 0 & J_{24} & J_{34} & J_{44} \end{bmatrix} \tag{16j, k}$$

where the following definitions are employed:

$$J_{ij} = e\int_S \left(\overline{g}_i^{(a)}\overline{g}_j^{(a)}\right)\mathrm{d}s + \frac{e^3}{12}\int_S \left(\overline{g}_i^{(d)}\overline{g}_j^{(d)}\right)\mathrm{d}s \tag{17a}$$

$$\overline{\lambda}_y = \int_0^s Z(s)\,\mathrm{d}s + \frac{\alpha}{S}\oint \mathrm{d}s\int_0^s Z(s)\,\mathrm{d}s \tag{17b}$$

$$\overline{\lambda}_z = \int_0^s Y(s)\,\mathrm{d}s + \frac{\alpha}{S}\oint \mathrm{d}s\int_0^s Y(s)\,\mathrm{d}s \tag{17c}$$

$$\overline{\lambda}_\omega = \int_0^s \omega_P(s)\,\mathrm{d}s + \frac{\alpha}{S}\oint \mathrm{d}s\int_0^s \omega_P(s)\,\mathrm{d}s \tag{17d}$$

with

$$\overline{g}^{(a)} = \langle 1, Z(s), Y(s), \omega_P(s), \psi(s)\rangle,$$

$$\overline{g}^{(d)} = \left\langle 0, \frac{\mathrm{d}Y}{\mathrm{d}s}, -\frac{\mathrm{d}Z}{\mathrm{d}s}, l(s), 2 \right\rangle \tag{18}$$

In expressions (17b)–(17d) the coefficient α can have the value 0 or 1 depending on whether the cross-section contour is open or closed, respectively. S denotes the contour perimeter.

The selected field of shell stress resultants (14) verifies expressions (13) in addition to the following shell equilibrium equations:

Table 1
Convergence of the element for buckling and lateral buckling loads of clamped–free closed section beam

Number of elements	Axial buckling load Q_X [N]	Lateral buckling load Q_Z [N]
1	454,890	243,922
2	444,268	186,978
5	441,634	165,998
10	441,271	163,473
15	441,204	162,996
20	441,181	162,824
30	441,164	162,700

Table 2
Comparison of buckling loads for a pinned–pinned closed section beam

Sequence	Model	Method	h/L			
			0.05	0.10	0.15	0.20
0/0/0/0	No shear	FEM	5.23	20.86	46.96	81.45
	flexible	Analytic	5.21	20.84	46.89	81.36
	Shear	FEM	4.41	12.00	17.59	21.02
	flexible	Analytic	4.39	11.98	17.54	20.97
0/90/90/0	No shear	FEM	2.81	11.27	25.20	44.43
	flexible	Analytic	2.79	11.17	25.14	44.39
	Shear	FEM	2.57	8.06	13.33	17.30
	flexible	Analytic	2.54	7.99	13.25	17.23
45/−45/−45/45	No shear	FEM	0.55	2.17	4.85	8.58
	flexible	Analytic	0.54	2.17	4.88	8.59
	Shear	FEM	0.54	2.16	4.77	8.30
	flexible	Analytic	0.54	2.15	4.77	8.30

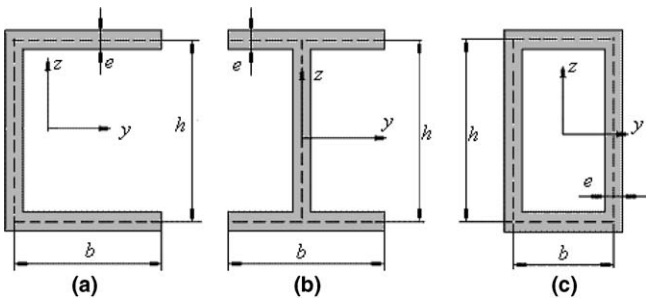

Fig. 3. Cross-sections analyzed. (a) $b = h = 0.1$ m, (b) $b = h = 0.1$ m, (c) $b = h/2 = 0.1$ m. The thickness is $e = 0.01$ m in the three cases.

$$\frac{\partial N_{xx}}{\partial x}+\frac{\partial N_{xs}}{\partial s}=0 \tag{19a}$$

$$\frac{\partial M_{xx}}{\partial x}+\frac{\partial M_{xs}}{\partial s}-N_{xn}=0 \tag{19b}$$

Substituting expressions (14) and (15) into (1b), integrating with respect to variable "s" and taking variations with respect to Q_X, M_Y, M_Z, B, T_{SV}, Q_Z, Q_Y and T_W one obtains, after some algebraic manipulation, the following constitutive equations for the beam stress resultants:

$$\boldsymbol{Q}_N = E^*\boldsymbol{J}_N^*\boldsymbol{\varepsilon}_N \tag{20a}$$

$$\boldsymbol{Q}_T = G^*\left(\boldsymbol{J}_T^*\right)^{\mathrm{T}}\left(\boldsymbol{C}_Q\right)^{-1}\boldsymbol{J}_T^*\boldsymbol{\varepsilon}_T = G^*\boldsymbol{S}\boldsymbol{\varepsilon}_T \tag{20b}$$

where $\boldsymbol{S}$ is the shear stiffness matrix and

$$\boldsymbol{C}_Q = \boldsymbol{C}_{N3}\boldsymbol{C}_{N3}^{\mathrm{T}}+\frac{e^4\overline{A}_{66}}{144\overline{A}_{55}^{(H)}}\boldsymbol{C}_{N2}\boldsymbol{C}_{N2}^{\mathrm{T}}+\frac{G^*}{12G^{**}}\boldsymbol{C}_{N5}\boldsymbol{C}_{N5}^{\mathrm{T}} \tag{21}$$

and E^*, G^* and G^{**} are expressed in the form:

$$E^*=\frac{\overline{A}_{11}}{e},\quad G^*=\frac{\overline{A}_{66}}{e} \tag{22a, b}$$

$$G^{**}=\begin{cases} G^* & \text{for closed sections} \\ \dfrac{12\overline{D}_{66}}{e^3} & \text{for open sections} \end{cases} \tag{22c}$$

The constitutive form (20) is a generalization of that obtained by Cortínez and Piovan [16]. The present beam model is governed by expressions (12) and (20) along with corresponding boundary conditions.

3. Finite element analysis

In order to obtain the buckling loads of the thin-walled shear deformable beams, a finite element is formulated based on the present theory. The element has two nodes with seven degrees of freedom in each one, and constitutes an extension of the element developed by Cortínez and Rossi [15] for isotropic materials.

Table 3
Buckling loads (Q_X [N]) for a U-section beam with different stacking sequences, slenderness ratios and boundary conditions

Boundary conditions	Stacking sequence	Model	$h/L=0.05$	$h/L=0.10$	$h/L=0.15$	$h/L=0.20$
SS–SS	0/0/0/0	[I]	2.674(XZ)	9.501(XZ)	20.828(XZ)	36.588(XZ)
		[II]	2.491(XZ)	7.323(XZ)	12.451(XZ)	16.655(XZ)
		[III]	6.833	22.925	40.219	54.480
	0/90/90/0	[I]	1.635(XZ)	5.370(XZ)	11.559(XZ)	20.169(XZ)
		[II]	1.572(XZ)	4.625(XZ)	8.468(XZ)	12.223(XZ)
		[III]	3.835	13.881	26.742	39.398
	45/−45/−45/45	[I]	1.235(Y)	2.750(XZ)	4.129(XZ)	5.843(XZ)
		[II]	1.232(Y)	2.736(XZ)	4.097(XZ)	5.770(XZ)
		[III]	0.197	0.526	0.795	1.249
C–C	0/0/0/0	[I]	9.503(XZ)	36.595(XZ)	81.028(XZ)	141.769(XZ)
		[II]	7.453(XZ)	16.891(XZ)	22.237(XZ)	25.004(XZ)
		[III]	21.572	53.844	72.557	82.363
	0/90/90/0	[I]	5.371(XZ)	20.173(XZ)	44.444(XZ)	77.619(XZ)
		[II]	4.704(XZ)	12.429(XZ)	18.348(XZ)	22.048(XZ)
		[III]	12.426	38.388	58.717	71.595
	45/−45/−45/45	[I]	2.750(XZ)	5.844(XZ)	10.512(XZ)	16.832(XZ)
		[II]	2.745(XZ)	5.828(XZ)	10.367(XZ)	16.291(XZ)
		[III]	0.197	0.269	1.376	3.215
C–SS	0/0/0/0	[I]	5.058(XZ)	18.982(XZ)	41.995(XZ)	73.819(XZ)
		[II]	4.369(XZ)	11.436(XZ)	16.858(XZ)	20.314(XZ)
		[III]	13.617	39.753	59.857	72.481
	0/90/90/0	[I]	2.941(XZ)	10.551(XZ)	23.123(XZ)	40.506(XZ)
		[II]	2.613(XZ)	7.312(XZ)	12.508(XZ)	16.729(XZ)
		[III]	11.159	30.694	45.905	58.699
	45/−45/−45/45	[I]	2.005(XZ)	3.920(XZ)	6.418(XZ)	9.759(XZ)
		[II]	1.997(XZ)	3.900(XZ)	6.347(XZ)	9.550(XZ)
		[III]	0.396	0.535	1.106	2.145
C–F	0/0/0/0	[I]	0.947(XZ)	2.674(XZ)	5.522(XZ)	9.501(XZ)
		[II]	0.926(XZ)	2.481(XZ)	4.715(XZ)	7.291(XZ)
		[III]	2.236	7.206	14.620	23.261
	0/90/90/0	[I]	0.670(XZ)	1.635(XZ)	3.195(XZ)	5.370(XZ)
		[II]	0.658(XZ)	1.572(XZ)	2.893(XZ)	4.654(XZ)
		[III]	1.680	3.827	9.463	13.335
	45/−45/−45/45	[I]	0.309(Y)	1.234(XZ)	2.100(XZ)	2.750(XZ)
		[II]	0.309(Y)	1.232(XZ)	2.090(XZ)	2.733(XZ)
		[III]	0.000	0.165	0.485	0.621

[I] Model neglecting shear flexibility. [II] Model allowing for shear flexibility. [III] Percentage difference: $100(Q_{X[II]}-Q_{X[I]})/Q_{X[II]}$. (SS) Simply supported, (C) clamped, (F) free.

The generalized nodal displacements may be written as

$$w = \left\langle u_{xc_1}, u_{yc_1}, \theta_{z_1}, u_{zc_1}, \theta_{y_1}, \phi_{x_1}, \theta_{x_1}, u_{xc_2}, u_{yc_2}, \theta_{z_2}, u_{zc_2}, \theta_{y_2}, \phi_{x_2}, \theta_{x_2} \right\rangle^{\mathrm{T}} \tag{23}$$

while the displacement field in the element is interpolated in the form:

$$u_{xc} = a_0 + a_1\tilde{x}, \quad u_{yc} = b_0 + b_1\tilde{x} + b_2\tilde{x}^2 + b_3\tilde{x}^3,$$

$$\theta_z = b_1 + \frac{\beta_1 b_3}{2} + 2b_2\tilde{x} + 3b_3\tilde{x}^2 \tag{24a, b, c}$$

$$u_{zc} = c_0 + c_1\tilde{x} + c_2\tilde{x}^2 + c_3\tilde{x}^3, \quad \theta_y = c_1 + \frac{\beta_2 c_3}{2} + 2c_2\tilde{x} + 3c_3\tilde{x}^2 \tag{24d, e}$$

$$\phi_x = d_0 + d_1\tilde{x} + d_2\tilde{x}^2 + d_3\tilde{x}^3, \quad \theta_x = d_1 + \frac{\beta_3 d_3}{2} + 2d_2\tilde{x} + 3d_3\tilde{x}^2 \tag{24f, g}$$

where the coefficients a_is , b_is , c_is and d_is are indeterminate constants whereas

$$\tilde{x} = \frac{x}{l_e}; \quad \beta_1 = \frac{12E^*J_{22}}{G^*S_{22}l_e^2}; \quad \beta_2 = \frac{12E^*J_{33}}{G^*S_{33}l_e^2}; \quad \beta_1 = \frac{12E^*J_{44}}{G^*S_{44}l_e^2} \tag{25a, b, c, d}$$

It must be noted that this interpolation yields:

$$\frac{\partial u_{yc}}{\partial x} - \theta_z = -\frac{\beta_1 b_3}{2}; \quad \frac{\partial u_{zc}}{\partial x} - \theta_y = -\frac{\beta_2 c_3}{2}; \quad \frac{\partial \phi_x}{\partial x} - \theta_x = -\frac{\beta_3 d_3}{2} \tag{26a, b, c, d}$$

It may be easily seen that when the coefficients β_i ($i = 1, 2, 3$) are very small (i.e. slender beams), expressions (26) become zero. Therefore this element avoids the shear-locking phenomenon. On the other hand it is possible to use the present element as a Vlasov-type beam element, which may be obtained from the present one as a limiting case, by taking large values to the shear coefficient (G^*S_{ii}) in the element stiffness matrix, in order to neglect the shear effect.

Table 4
Buckling loads (Q_X [N]) for a I-section beam with different stacking sequences, slenderness ratios and boundary conditions

Boundary conditions	Stacking sequence	Model	$h/L = 0.05$	$h/L = 0.10$	$h/L = 0.15$	$h/L = 0.20$
SS–SS	0/0/0/0	[I]	5.943(Y)	23.474(Y)	52.910(Y)	93.179(Y)
		[II]	5.548(Y)	18.454(Y)	32.438(Y)	36.811(Z)
		[III]	6.651	21.385	38.692	60.494
	0/90/90/0	[I]	3.197(Y)	12.734(Y)	28.470(Y)	50.114(Y)
		[II]	3.098(Y)	11.008(Y)	21.552(Y)	30.890(Y)
		[III]	3.082	13.553	24.299	38.361
	45/−45/−45/45	[I]	0.620(Y)	2.468(Y)	5.515(Y)	9.713(Y)
		[II]	0.619(Y)	2.458(Y)	5.468(Y)	9.569(Y)
		[III]	0.098	0.387	0.855	1.484
C–C	0/0/0/0	[I]	23.681(Y)	93.198(Y)	204.215(Y)	350.235(Y)
		[II]	18.537(Y)	36.900(Z)	39.270(Z)	40.177(Z)
		[III]	21.721	60.407	80.770	88.529
	0/90/90/0	[I]	12.736(Y)	50.125(Y)	109.834(Y)	188.369(Y)
		[II]	11.156(Y)	31.156(Y)	35.087(Z)	38.152(Z)
		[III]	12.408	37.843	68.055	79.746
	45/−45/−45/45	[I]	2.468(Y)	9.715(Y)	21.287(Y)	36.509(Y)
		[II]	2.459(Y)	9.574(Y)	20.639(Y)	34.702(Y)
		[III]	0.378	1.449	3.044	4.950
C–SS	0/0/0/0	[I]	12.142(Y)	48.163(Y)	106.883(Y)	186.445(Y)
		[II]	10.471(Y)	29.578(Y)	34.487(Z)	37.534(Z)
		[III]	13.759	38.587	67.734	79.869
	0/90/90/0	[I]	6.530(Y)	25.904(Y)	57.486(Y)	100.277(Y)
		[II]	6.157(Y)	19.987(Y)	31.446(Z)	36.458(Z)
		[III]	5.715	22.841	45.298	63.643
	45/−45/−45/45	[I]	1.266(Y)	5.020(Y)	11.141(Y)	19.435(Y)
		[II]	1.263(Y)	4.978(Y)	10.936(Y)	18.829(Y)
		[III]	0.218	0.851	1.845	3.119
C–F	0/0/0/0	[I]	1.487(Y)	5.943(Y)	13.349(Y)	23.676(Y)
		[II]	1.461(Y)	5.546(Y)	11.503(Y)	18.435(Y)
		[III]	1.770	6.684	13.831	22.135
	0/90/90/0	[I]	0.800(Y)	3.196(Y)	7.180(Y)	12.734(Y)
		[II]	0.791(Y)	3.057(Y)	6.512(Y)	10.777(Y)
		[III]	1.133	4.371	9.301	15.366
	45/−45/−45/45	[I]	0.155(Y)	0.619(Y)	1.391(Y)	2.468(Y)
		[II]	0.155(Y)	0.619(Y)	1.388(Y)	2.458(Y)
		[III]	0.000	0.000	0.221	0.390

[I] Model neglecting shear flexibility. [II] Model allowing for shear flexibility. [III] Percentage difference: 100 ($Q_{X[II]} - Q_{X[I]}$)/$Q_{X[II]}$. (SS) Simply supported, (C) clamped, (F) free.

Table 5
Buckling loads (Q_X [N]) for a closed-section beam with different stacking sequences, slenderness ratios and boundary conditions

Boundary conditions	Stacking sequence	Model	$h/L = 0.05$	$h/L = 0.10$	$h/L = 0.15$	$h/L = 0.20$
SS–SS	0/0/0/0	[I]	5.235(Y)	20.863(Y)	46.664(Y)	81.446(X)
		[II]	4.651(Y)	13.912(Y)	22.041(Y)	27.708(Y)
		[III]	11.148	33.318	52.766	65.980
	0/90/90/0	[I]	2.810(Y)	11.267(Y)	25.201(Y)	44.432(X)
		[II]	2.681(Y)	9.152(Y)	15.142(Y)	19.285(Y)
		[III]	4.591	18.773	39.915	56.597
	45/−45/−45/45	[I]	0.546(Y)	2.175(Y)	4.854(Y)	8.576(Y)
		[II]	0.544(Y)	2.156(Y)	4.774(Y)	8.301(Y)
		[III]	0.213	0.846	1.659	3.211
C–C	0/0/0/0	[I]	20.867(Y)	81.448(X)	88.478(X)	98.284(X)
		[II]	13.988(Y)	27.858(Y)	34.066(Y)	36.934(Y)
		[III]	32.967	65.796	61.498	62.421
	0/90/90/0	[I]	11.270(Y)	44.411(Y)	82.877(X)	88.348(X)
		[II]	9.152(Y)	18.875(Y)	24.821(Y)	27.365(Y)
		[III]	18.790	57.499	70.051	69.026
	45/−45/−45/45	[I]	2.175(Y)	8.578(Y)	18.857(Y)	32.477(Y)
		[II]	2.157(Y)	8.309(Y)	17.627(Y)	29.071(Y)
		[III]	0.825	3.138	6.523	10.489
C–SS	0/0/0/0	[I]	10.696(Y)	42.471(Y)	82.295(X)	87.329(X)
		[II]	8.356(Y)	20.118(Y)	27.301(Y)	31.360(Y)
		[III]	21.874	52.631	66.826	64.090
	0/90/90/0	[I]	5.776(Y)	22.936(Y)	50.987(Y)	82.235(X)
		[II]	4.972(Y)	14.250(Y)	19.874(Y)	26.125(Y)
		[III]	13.923	37.872	61.022	68.231
	45/−45/−45/45	[I]	1.115(Y)	4.427(Y)	9.842(Y)	17.207(Y)
		[II]	1.110(Y)	4.345(Y)	9.450(Y)	16.060(Y)
		[III]	0.475	1.850	3.980	6.665
C–F	0/0/0/0	[I]	1.310(Y)	5.234(Y)	11.760(Y)	20.863(Y)
		[II]	1.269(Y)	4.648(Y)	9.168(Y)	13.893(Y)
		[III]	3.115	11.204	22.041	33.408
	0/90/90/0	[I]	0.707(Y)	2.827(Y)	6.351(Y)	11.297(Y)
		[II]	0.695(Y)	2.684(Y)	5.359(Y)	8.984(Y)
		[III]	1.747	5.055	15.620	20.474
	45/−45/−45/45	[I]	0.137(Y)	0.546(Y)	1.226(Y)	2.175(Y)
		[II]	0.136(Y)	0.544(Y)	1.220(Y)	2.156(Y)
		[III]	0.051	0.216	0.482	0.850

[I] Model neglecting shear flexibility. [II] Model allowing for shear flexibility. [III] Percentage difference: $100\,(Q_{X[II]} - Q_{X[I]})/Q_{X[II]}$. (SS) Simply supported, (C) clamped, (F) free.

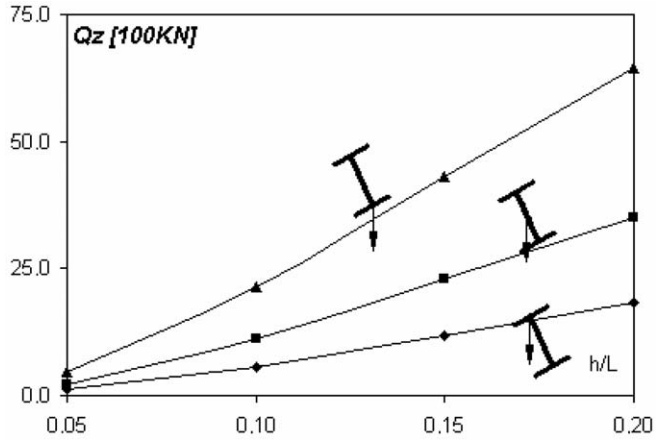

Fig. 4. Variation of lateral buckling load with respect to slenderness ratio, for a composite clamped–clamped I-beam with stacking sequence {0/90/90/0}.

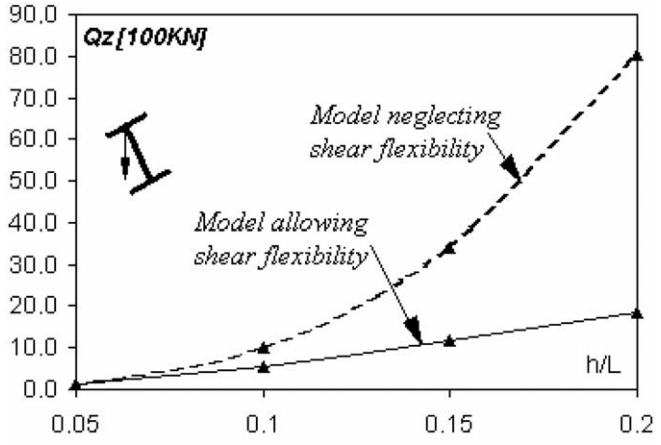

Fig. 5. Lateral buckling loads of a composite clamped–clamped I-beam with stacking sequence {0/90/90/0}. Comparison of models neglecting and allowing shear flexibility.

Substituting (23) into the governing variational Eq. (11) and assembling in the usual way, one arrives to

$$(\boldsymbol{K} + \lambda \boldsymbol{K}_{\mathrm{G}})\boldsymbol{W}^{*} = 0 \tag{27}$$

where $\boldsymbol{K}$, $\boldsymbol{K}_{\mathrm{G}}$, and W^{*} are the global stiffness, global geometric stiffness matrices and the global displacement vector respectively. In order to calculate the eigenvalues, it is necessary to obtain the prebuckling state by solving the self-equilibrating system of initial stresses and, initial volume and surface forces (see references [24,25,27]).

4. Numerical examples and discussion

In order to evaluate the shear effect on the stability behavior of the analyzed structural members, numerical comparisons are performed among the present model predictions and results obtained by neglecting the shear deformability (Ghorbanpoor and Omidvar, [9], and Lee et al. [12–14]). Different cross-sectional shapes, laminate schemes and slenderness ratios are considered. The analyzed material is graphite-epoxy (AS4/3501) whose properties are $E_1 = 144$ GPa, $E_2 = 9.65$ GPa, $G_{12} = 4.14$ GPa, $G_{13} = 4.14$ GPa, $G_{23} = 3.45$ GPa, $v_{12} = 0.3$, $v_{13} = 0.3$, $v_{23} = 0.5$, $\rho = 1389$ kg/m^3. The considered laminate schemes are: (a) {0/0/0/0}, (b) {0/90/90/0} and (c) {45/−45/−45/45}. The analyzed cross-sections are shown in Fig. 3.

4.1. Convergence analysis and comparisons

In Table 1, it is presented a convergence analysis for buckling and lateral buckling of a clamped–free beam with a closed rectangular section, with $h/L = 0.1$, $\{h, b, e\} = \{0.1, 0.5, 0.01\}$ m, and stacking sequence of {0/0/0/0}. On the other hand, in Table 2 a comparison with analytical results [16] of buckling loads for a pinned–pinned beam with closed section is shown. Different stacking sequences and slenderness ratios were considered. In Table 2 models with 30 finite elements were employed. From these tables, it is possible to note a fast convergence as well as good agreement with analytical results.

4.2. Buckling problems

In Tables 3–5, comparisons of buckling loads, of shear flexible and non-shear flexible models for U-section, I-section and closed section are presented. In these tables, the eigenvalues (buckling loads) are normalized with respect to 10^5 and the capital letters (Y), (Z), (X) and (XZ) are employed, in order to indicate the corresponding buckling mode. In this way, (Y), (Z), (X) and (XZ) stand for flexural mode in y-direction, flexural mode in z-direction, torsional mode and flexural torsional mode (characteristic of monosymmetric cross-sections), respectively.

In Tables 3–5, it is possible to see the strong influence of shear flexibility in laminates {0/0/0/0} and {0/90/90/0}, which increases with the slenderness ratio h/L. In this sense the percentage differences can reach 88.529% for clamped–clamped I-beams with a {0/0/0/0} stacking sequence (see Table 4, $h/L = 0.20$). Also, it is possible to note that buckling modes are dominant flexural torsional in the U-beams and dominant flexural in y-direction, for beams with the other two types of cross-section. The influence of shear flexibility is also observed in the change of the buckling mode shape, as it can be seen, for example, in Table 5, in the case of a clamped–clamped boundary condition, laminates {0/0/0/0} or {0/90/90/0} with $h/L = 0.15$ or higher. These tables were obtained with models of 30 finite elements.

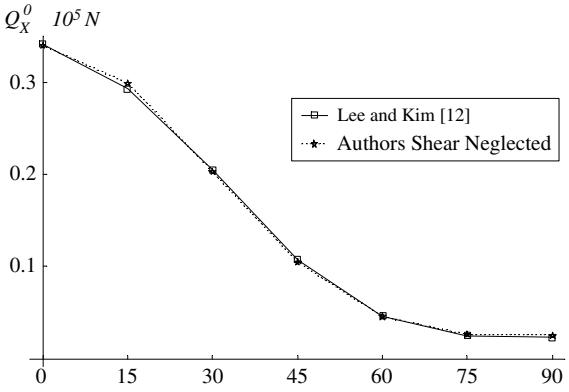

Fig. 6. Buckling loads of a composite simply supported I-beam with stacking sequence {α/−α/α/α}. Comparison of the present model (reduced neglecting shear flexibility) with other models.

4.3. Lateral buckling problems

In Fig. 4, the variation of the lateral buckling load with respect to the slenderness ratio is depicted. This case, performed with the shear flexible model, corresponds to a clamped–clamped I-beam with stacking sequence {0/90/90/0}, carrying a point load at the middle of the beam. On the other hand, in Fig. 5, a comparison of lateral buckling loads between models allowing and neglecting shear flexibility is performed. It is possible to see a strong influence of shear effects in the prediction of lateral buckling loads, especially at large slenderness ratios (i.e. h/L). The aforementioned figures were obtained with models of 30 finite elements.

4.4. Comparisons

In order to check the efficiency of the introduced theory, in the present section comparisons with the theories of Lee and Kim [12], Sherbourne and Kabir [7] and with shell models of COSMOS/M are performed. In these comparisons, models with 30 finite elements of the present beam theory are employed.

The model of Lee and Kim [12] is compared with the present theory neglecting the shear flexibility in the Fig. 6. This Figure shows buckling loads due to compressive loads (applied at both ends) for a simple supported composite I-beam with stacking sequence {α/−α/−α/α} in

Table 6
Lateral buckling loads (concentrated load Q_Z [kN] in $x = L/2$, applied at the centroid) for a simply supported composite I-beam (flanges—fiber-angle $\alpha = 0°$, web lamination $\{\alpha/-\alpha/-\alpha/\alpha\}$)

Web fiber angle, α	Allowing shear flexibility			Neglecting shear flexibility		
	[I]	[II]	[III]	[I]	[II]	[III]
0	82.1	83.4	1.57	88.4	89.2	0.96
10	84.1	85.5	1.66	90.3	91.3	1.07
20	89.0	90.4	1.63	95.2	96.4	1.17
30	93.3	94.4	1.15	100.2	101.5	1.36
40	96.2	95.1	1.22	103.2	102.2	0.98
45	96.5	95.0	1.49	103.4	102.1	1.20

[I] Model of Sherbourne and Kabir [30]. [II] Authors model. [III] Percentage difference: $100|Q_{Z[I]} - Q_{Z[II]}|/Q_{Z[I]}$.

Table 7
Comparisons of buckling loads (Q_X) and lateral buckling loads (Q_Z) of a cantilever I-beam, obtained with the present shear deformable beam theory and finite element shell models of COSMOS/M

Type of load	Material	Type of model	Value [N]
Q_Z	Steel	Beam theory	85,045
		Shell8T (COSMOS/M)	81,643
		Difference [%]	4.16%
Q_X	Steel	Beam theory	112,082
		Shell8T (COSMOS/M)	109,840
		Difference [%]	2.04%
Q_X	AS4/3501-6 {0/90/90/0}	Beam theory	41,861
		Shell8T (COSMOS/M)	40,698
		Difference [%]	2.85%
Q_X	AS4/3501-6 {45/−45/−45/45}	Beam theory	8012
		Shell8T (COSMOS/M)	7958
		Difference [%]	0.68%

The difference [%] is taken with respect to the load values of the shell models.

both the web and flanges. The beam has the following dimensions: length 800 cm, web height 20 cm, flange width 10 cm and thickness 1 cm. The composite material is a graphite-epoxy with $E_{11} = 133.4$ GPa, $E_{22} = 8.78$ GPa, $G_{12} = 3.67$ GPa and $\nu_{12} = 0.26$. As one can see, the present theory can be reduced to the Lee and Kim [12] model.

Sherbourne and Kabir, in their theory, considered only the shear flexibility due to bending, whereas they neglected the shear flexibility due to non-uniform torsion warping. Also the virtual work terms due to off-axis forces were not taken into account by Sherbourne and Kabir. In this context, the authors' model can be reduced to the Sherbourne and Kabir model, by neglecting the aforementioned components.

Table 6 offers the critical loads for the lateral buckling of a simply supported I-beam, whose flanges have a fiber orientation $\alpha = 0°$ and the web has the stacking sequence $\{\alpha/-\alpha/-\alpha/\alpha\}$. The loading scheme is composed by a point load applied in the web direction and located at the midspan in the cross-sectional centroid, i.e. $\{x, y, z\} = \{L/2, 0, 0\}$. The cross-section dimensions are $\{h, b, e\} = \{20.32, 10.16, 0.953\}$ cm., the beam has a length $L = 12h$, and the material properties can be found in Reference [7]. As one can see in Table 6, the reduced model of the authors agrees well (with less that 1.70%) with the model of Sherbourne and Kabir, both, allowing or neglecting the shear flexibility components.

Finally Table 7 shows a comparison of the present shear deformable beam theory with shell models of the finite element program COSMOS/M for an isotropic and orthotropic cantilever I-beam. The materials are steel ($E = 210$ GPa, $G = 80.76$ GPa) and Graphite-Epoxy AS4/3501-6 ($E_{11} = 144$ GPa, $E_{22} = 9.68$ GPa, $G_{12} = 4.14$ GPa, $G_{23} = 3.45$ GPa, $\nu_{12} = 0.3$, $\nu_{23} = 0.48$). The beam has the following dimensions: length 100 cm, web height 10 cm, flanges width 5 cm and overall thickness 1 cm. Two types of loads are considered. The first is a lateral load Q_Z applied in the cross-sectional center at the free end in the web direction. The second is a compressive load Q_X applied in the cross-sectional center at the free end. For this comparison models with more than 12000 shell elements (SHELL8T) were employed to calculate the buckling loads in COSMOS/M. In Table 7 one can see a good agreement of buckling loads obtained with the present theory and with finite element shell models.

5. Conclusions

A new model for general stability analysis of shearable thin-walled composite beams has been presented in this paper. This model constitutes a generalization of that proposed by the authors in Ref. [16].

The generalization consists in the adoption of an enhanced displacement field with non-linear terms based on the rule of semi-tangential rotations. On the other hand, the model takes into account an arbitrary state of initial stresses.

In order to solve the governing variational equation, a non-locking finite element with fourteen degrees of freedom was employed. The numerical results demonstrate that the shear flexibility has a remarkable effect on the critical loads, especially when one of the material axes coincides with the longitudinal axis of the beam.

Acknowledgements

The present study was sponsored by Secretaría de Ciencia y Tecnología de Universidad Tecnológica Nacional, Research Project 25/B008 and by CONICET (National Council of Scientific and Technological Research).

Appendix I

The constitutive equations of symmetric balanced laminates may be expressed in terms of shell stress resultants in the following form [1]:

$$\begin{Bmatrix} N_{xx} \\ N_{xs} \\ N_{xn} \\ M_{xx} \\ M_{xs} \end{Bmatrix} = \begin{bmatrix} \overline{A}_{11} & 0 & 0 & 0 & 0 \\ 0 & \overline{A}_{66} & 0 & 0 & 0 \\ 0 & 0 & \overline{A}_{55}^{(H)} & 0 & 0 \\ 0 & 0 & 0 & \overline{D}_{11} & 0 \\ 0 & 0 & 0 & 0 & \overline{D}_{66} \end{bmatrix} \begin{Bmatrix} \varepsilon_{xx}^{L} \\ \gamma_{xs}^{L} \\ \gamma_{xn}^{L} \\ \kappa_{xx}^{L} \\ \kappa_{xs}^{L} \end{Bmatrix} \tag{A.I.1}$$

with

$$\overline{A}_{11} = A_{11} - \frac{A_{12}^2}{A_{22}}, \quad \overline{A}_{66} = A_{66} - \frac{A_{26}^2}{A_{22}},$$

$$\overline{A}_{55}^{(H)} = A_{55}^{(H)} - \frac{\left(A_{45}^{(H)}\right)^2}{A_{44}^{(H)}} \tag{A.I.2.a, b, c}$$

$$\overline{D}_{11} = D_{11} - \frac{D_{12}^2}{D_{22}}, \quad \overline{D}_{66} = D_{66} - \frac{D_{26}^2}{D_{22}} \tag{A.I.2.d, e}$$

where A_{ij}, D_{ij} and $A_{ij}^{(H)}$ are plate stiffness coefficients defined according to the lamination theory presented in reference [1, chapter 6]. The coefficient $\overline{D}_{16}$ has been neglected, because of its low value for the considered laminate stacking sequence.

Appendix II

The initial forces expressions due to initial volume forces and initial surface forces, which were introduced in (12c), are now defined extensively in the following form:

(1) Volume initial forces:

$$\overline{X}_3^{(0)} = -N_1^{(0)}\theta_z - \frac{N_3^{(0)} + N_4^{(0)}}{2}\theta_y + \frac{N_6^{(0)}}{2}\phi_x \tag{A.II.1}$$

$$\overline{X}_5^{(0)} = -\frac{N_3^{(0)} + N_4^{(0)}}{2}\theta_z - N_2^{(0)}\theta_y - \frac{N_5^{(0)}}{2}\phi_x \tag{A.II.2}$$

$$\overline{X}_6^{(0)} = \frac{N_6^{(0)}}{2}\theta_z - \frac{N_5^{(0)}}{2}\theta_y - \left(N_1^{(0)} + N_2^{(0)}\right)\phi_x \tag{A.II.3}$$

with

$$\left\{N_1^{(0)}, N_2^{(0)}, N_3^{(0)}\right\} = \int_A \left\{y\overline{X}_y^{(0)}, z\overline{X}_z^{(0)}, y\overline{X}_z^{(0)}\right\} \mathrm{d}s\,\mathrm{d}n \tag{A.II.4}$$

$$\left\{N_4^{(0)}, N_5^{(0)}, N_6^{(0)}\right\} = \int_A \left\{z\overline{X}_y^{(0)}, y\overline{X}_x^{(0)}, z\overline{X}_x^{(0)}\right\} \mathrm{d}s\,\mathrm{d}n \tag{A.II.5}$$

(2) Surface initial forces:

$$\overline{T}_3^{(0)} = -H_1^{(0)}\theta_z - \frac{H_3^{(0)} + H_4^{(0)}}{2}\theta_y + \frac{H_6^{(0)}}{2}\phi_x \tag{A.II.6}$$

$$\overline{T}_5^{(0)} = -\frac{H_3^{(0)} + H_4^{(0)}}{2}\theta_z - H_2^{(0)}\theta_y - \frac{H_5^{(0)}}{2}\phi_x \tag{A.II.7}$$

$$\overline{T}_6^{(0)} = \frac{H_6^{(0)}}{2}\theta_z - \frac{H_5^{(0)}}{2}\theta_y - \left(H_1^{(0)} + H_2^{(0)}\right)\phi_x \tag{A.II.8}$$

with

$$\left\{H_1^{(0)}, H_2^{(0)}, H_3^{(0)}\right\} = \int_A \left\{y\overline{T}_y^{(0)}, z\overline{T}_z^{(0)}, y\overline{T}_z^{(0)}\right\} \mathrm{d}s\,\mathrm{d}n \tag{A.II.9}$$

$$\left\{H_4^{(0)}, H_5^{(0)}, H_6^{(0)}\right\} = \int_A \left\{z\overline{T}_y^{(0)}, y\overline{T}_x^{(0)}, z\overline{T}_x^{(0)}\right\} \mathrm{d}s\,\mathrm{d}n \tag{A.II.10}$$

(3) Consider an initial point-load $\overline{F}^{(0)} = \left\{\overline{F}_x^{(0)}, \overline{F}_y^{(0)}, \overline{F}_z^{(0)}\right\}$, applied at an off-axis point $\boldsymbol{B}(x_B, y_B, z_B)$, as it is shown in the Fig. 1b. Now, applying Delta–Kronecker multipliers at the point $\boldsymbol{B}$, the virtual work term for the off-axis forces can be expressed as

$$L_{KG22} = -\left[\overline{T}_3^{(0)}\delta\theta_z + \overline{T}_5^{(0)}\delta\theta_y + \overline{T}_6^{(0)}\delta\phi_x\right]_{x=x_B} \tag{A.II.11}$$

where

$$\overline{T}_3^{(0)} = -y_B\overline{F}_y^{(0)}\theta_z - \frac{z_B\overline{F}_y^{(0)} + y_B\overline{F}_z^{(0)}}{2}\theta_y + \frac{z_B\overline{F}_x^{(0)}}{2}\phi_x \tag{A.II.12}$$

$$\overline{T}_5^{(0)} = -\frac{z_B\overline{F}_y^{(0)} + y_B\overline{F}_z^{(0)}}{2}\theta_z - z_B\overline{F}_z^{(0)}\theta_y - \frac{y_B\overline{F}_x^{(0)}}{2}\phi_x \tag{A.II.13}$$

$$\overline{T}_6^{(0)} = \frac{z_B\overline{F}_x^{(0)}}{2}\theta_z - \frac{y_B\overline{F}_x^{(0)}}{2}\theta_y - \left(y_B\overline{F}_y^{(0)} + z_B\overline{F}_z^{(0)}\right)\phi_x \tag{A.II.14}$$

(4) The generalized beam stress resultants can be defined in terms of the shell stress resultants introduced in (A.I.1) by means of the following expressions:

$$Q_{YW}^{(0)} = \int_S \left(N_{xs}^{(0)}\frac{\mathrm{d}Y}{\mathrm{d}s} - N_{xn}^{(0)}\frac{\mathrm{d}Z}{\mathrm{d}s}\right)\omega_p\,\mathrm{d}s \tag{A.II.15}$$

$$Q_{ZW}^{(0)} = \int_S \left(N_{xs}^{(0)}\frac{\mathrm{d}Z}{\mathrm{d}s} + N_{xn}^{(0)}\frac{\mathrm{d}Y}{\mathrm{d}s}\right)\omega_p\,\mathrm{d}s \tag{A.II.16}$$

$$T_{WY}^{(0)} = \int_S \left(N_{xs}^{(0)}\frac{\mathrm{d}\omega}{\mathrm{d}s} + N_{xn}^{(0)}\frac{\mathrm{d}\omega}{\mathrm{d}n}\right)Y(s)\,\mathrm{d}s \tag{A.II.17}$$

$$T_{WZ}^{(0)} = \int_S \left(N_{xs}^{(0)}\frac{\mathrm{d}\omega}{\mathrm{d}s} + N_{xn}^{(0)}\frac{\mathrm{d}\omega}{\mathrm{d}n}\right)Z(s)\,\mathrm{d}s \tag{A.II.18}$$

$$T_{WW}^{(0)} = \int_S \left(N_{xs}^{(0)}\frac{\mathrm{d}\omega}{\mathrm{d}s} + N_{xn}^{(0)}\frac{\mathrm{d}\omega}{\mathrm{d}n}\right)\omega_p(s)\,\mathrm{d}s \tag{A.II.19}$$

Appendix III

When the cross-section axes are assumed to be the principal ones and a two-pole reference is employed, the forms (16) can be simplified and the field of the shell stress resultants can assumed to be of the form:

$$N_{xx} = e\left[\frac{N}{J_{11}} + \frac{M_y}{J_{22}}\overline{Z} + \frac{M_z}{J_{33}}\overline{Y} + \frac{B}{J_{44}}\omega_p\right] \tag{A.III.1}$$

$$M_{xx} = \frac{e^3}{12}\left[\frac{M_y}{J_{22}}\frac{\mathrm{d}Y}{\mathrm{d}s} - \frac{M_z}{J_{33}}\frac{\mathrm{d}Z}{\mathrm{d}s} + \frac{B}{J_{44}}l(s)\right] \tag{A.III.2}$$

$$M_{xs} = -\frac{e^3}{6J_{55}}T_{SV} \tag{A.III.3}$$

$$N_{xs} = e\left[-\frac{Q_z}{J_{22}}\overline{\lambda}_y(s) - \frac{Q_y}{J_{33}}\overline{\lambda}_z(s) - \frac{T_w}{J_{44}}\overline{\lambda}_w(s)\right] + \frac{e\psi}{J_{55}}T_{SV} \tag{A.III.4}$$

$$N_{xn} = \frac{e^3}{12}\left[\frac{Q_Z}{J_{22}}\frac{\mathrm{d}Y}{\mathrm{d}s} - \frac{Q_Y}{J_{33}}\frac{\mathrm{d}Z}{\mathrm{d}s} + \frac{T_W}{J_{44}}l(s)\right] \tag{A.III.5}$$

It is clear that, as defined in (17a) J_{11}, J_{22}, J_{33}, J_{44} and J_{55} are the cross-sectional area, second-order area moments, cross-sectional warping constant and St. Venant torsion constant, respectively.

Further explanations of the aforementioned expressions (A.III.1)–(A.III.5) can be found in Cortínez and Piovan [16] for composite materials or Vlasov [2] for isotropic materials.

References

[1] Barbero EJ. Introduction to composite material design. Taylor and Francis Inc; 1999.

[2] Vlasov VV. Thin walled elastic beams. Jerusalem: Israel Program for Scientific Translation; 1961.

[3] Bauld NR, Tzeng LS. A Vlasov theory for fiber-reinforced beams with thin-walled open cross sections. Int J Solids Struct 1984;20(3): 277–97.

[4] Ghorbanpoor A, Omidvar B. Simplified analysis of thin-walled composite members. J Struct Eng ASCE 1996;122(11):1379–83.

[5] Massa JC, Barbero EJ. A strength of materials formulation for thin-walled composite beams with torsion. J Compos Mater 1998;32(17): 1560–94.

[6] Pollock GD, Zak AR, Hilton HH, Ahmad MF. Shear center for elastic thin-walled composite beams. Struct Eng Mech 1995;3(1): 91–103.

[7] Sherbourne AN, Kabir MZ. Shear strains effects in lateral stability of thin-walled fibrous composite beams. J Eng Mech ASCE 1995; 121(5):640–7.

[8] Godoy LA, Barbero EJ, Raftoyiannis I. Interactive buckling analysis of fiber-reinforced thin-walled columns. J Compos Mater 1995; 29(5):591–613.

[9] Omidvar B. Shear coefficient in orthotropic thin-walled composite beams. J Compos Construction 1996;2(1):46–56.

[10] Librescu L, Song O. On the aeroelastic tailoring of composite aircraft swept wings modeled as thin walled beam structures. Compos Eng 1992;2(5–7):497–512.

[11] Bhaskar K, Librescu L. A Geometrically non-linear theory for laminated anisotropic thin-walled beams. Int J Eng Sci 1995;33(9): 1331–44.

[12] Lee J, Kim SE. Flexural-torsional buckling of thin-walled I-section composites. Comput Struct 2001;79:987–95.

[13] Lee J, Kim SE. Lateral buckling analysis of thin-walled laminated channel-section beams. Compos Struct 2002;56:391–9.

[14] Lee J, Kim SE, Hong K. Lateral buckling I-section beams. Eng Struct 2002;24:955–64.

[15] Cortínez VH, Rossi RE. Dynamics of shear deformable thin-walled open beams subjected to initial stresses. Rev Int Mét Num Cálculo y Diseño en Ingeniería 1998;14(3):293–316.

[16] Cortínez VH, Piovan MT. Vibration and buckling of composite thin-walled beams with shear deformability. J Sound Vib 2002; 258(4): 701–23.

[17] Wu XX, Sun CT. Vibration analysis of laminated composite thin-walled beams using finite elements. AIAA J 1990;29(5):736–42.

[18] Kollár LP. Flexural-torsional buckling of open section composite columns with shear deformation. Int J Solids Struct 2001;38:7525–41.

[19] Sapkás A, Kollár LP. Lateral-torsional buckling of composite beams. Int J Solids Struct 2001;39:2939–63.

[20] Chen WF, Lui EM. Structural stability. Theory and implementation. New York: Elsevier Science and Publishing; 1987.

[21] Timoshenko SP, Gere JM. Theory of elastic stability. 2nd ed. New York: McGraw Hill; 1961.

[22] Argyris JH, Hilpert O, Malejannakis GA, Scharpf DW. On the geometrical stiffness of a beam in space. Comput Methods Appl Mech Eng 1979;20:105–31.

[23] Argyris JH. An excursion into large rotations. Comput Methods Appl Mech Eng 1982;32:85–155.

[24] Kim MY, Chang SP, Park HG. Spatial postbuckling analysis of nonsymmetric thin-walled frames. I: Theoretical considerations based on the semitangential property. J Eng Mech 2001;127(8):769–78.

[25] Kim MY, Chang SP, Park HG. Spatial postbuckling analysis of nonsymmetric thin-walled frames. I: Geometrically nonlinear FE procedures. J Eng Mech 2001;127(8):779–90.

[26] Washizu K. Variational methods in elasticity and plasticity. New York: Pergamon Press; 1968.

[27] Piovan MT. Theoretical and computational study in the mechanics of composite thin walled curved beams, considering non-conventioanl effects [in spanish]. PhD thesis. Department of Engineering, Universidad Nacional del Sur. Bahía Blanca. Argentina, 2002.

[28] Krenk S, Gunneskov O. Statics of thin-walled pretwisted beams. Int J Numer Methods Eng 1981;17:1407–26.

[29] Conci A. Large displacements analysis of thin walled beams with generic open section. Int J Numer Methods Eng 1993;33:2109–27.

[30] Bathe KJ. Finite element procedures. NJ, USA: Prentice-Hall; 1996.